JOURNAL OF COMPUTATIONAL PHYSICS **138,** 121–152 (1997)
ARTICLE NO. CP975800

Solution of the Div-Curl Problem in Generalized Curvilinear Coordinates

F. Bertagnolio[1] and O. Daube[2]

LIMSI-CNRS, BP 133, 91403 Orsay Cedex, France
E-mail: franck@limsi.fr; daube@limsi.fr

Received December 9, 1996; revised July 7, 1997

We propose a method for solving the div-curl problem on a structured nonorthogonal curvilinear grid. The differential operators are discretized using a MAC-scheme for the unknowns in such a way that the discrete counterparts of the usual vector analysis relations are satisfied. The derived discrete problem is then solved by performing a Helmholtz-type decomposition of the unknown vector field. This allows us to obtain a vector field for which both divergence and curl are satisfied to within machine accuracy. The method is validated for several configurations in two and three dimensions, and its accuracy is numerically checked.

Key Words: div-curl problem; curvilinear coordinates; Navier–Stokes equations; velocity–vorticity formulation.

INTRODUCTION

In this paper we address the div-curl problem which consists of finding a vector field $\boldsymbol{v}$ assuming that its curl $\boldsymbol{\omega}$ and its divergence $\mathscr{D}$ are known. This problem, herafter denoted by DC, arises in many fields of physics, in particular in fluid mechanics and in electromagnetism. This work was carried out in the context of fluid mechanics, and more precisely, using the incompressible Navier–Stokes equations cast in the so-called velocity–vorticity formulation. In this Introduction we will therefore mainly refer to previous works which are relevant to fluid mechanics.

The main features of the velocity–vorticity formulation of the incompressible

[1] Present address: WEAPD, Bdg VEA-762, RISO National Laboratory, P.O. Box 49, DK-4000, Roskilde, Denmark

[2] Present address: CEMIF-Université d'Evry, 40 rue du Pelvoux, 91020 Evry Cedex, France

0021-9991/97 $25.00

Navier–Stokes equations will be outlined and for further details, the reader is referred to the book by Quartapelle [18] and the review paper by Gatski [8]. In this formulation the unknowns are the velocity $\boldsymbol{v}$ which is divergence free and the vorticity $\boldsymbol{\omega}$ which has to be the curl of $\boldsymbol{v}$. In all the published works, the resolution process reduces to a sequence of two elementary problems, the first of which consists of the resolution of a transport equation for the vorticity $\boldsymbol{\omega}$ with appropriate approximate boundary conditions, whereas the second one consists of the computation of the associated velocity field $\boldsymbol{v}$ using $\boldsymbol{\omega}$ as a source term.

In this paper we are concerned only with the last step for which most of the authors solve a vector Poisson equation. Only Gatski *et al.* [9] and Osswald *et al.* [16] solved directly the DC problem in its original first-order form. Another important point is that all these computations were performed on uniform cartesian grids, generally with a staggered MAC-scheme for the unknowns. In more recent works, Apanovich and Lyumkis [1] and Nicolaides [15] deal with unstructured meshes by means of covolume techniques which allow for a conservative discretization of the DC problem on two dual grids. The fact that these meshes are orthogonal to one another is the main feature of these techniques.

The goal of this paper is to treat the DC problem on general nonorthogonal structured grids. Numerical solutions of conservation law in curvilinear coordinates have already been widely studied. The crucial point for the numerical consistency turns out to be the choice of the basis on which the velocity is expressed. We refer to the paper of Shyy and Vu [21] for a review of different techniques which may be used for this purpose. In the case of discrete MAC grid (see Harlow and Welch [11]), the choice of covariant and contravariant components as dependant variables is natural. Unfortunately, whereas the use of such components is relatively simple in the case of orthogonal coordinates, many difficulties arise in the general case. Mainly, differentiating the basis vectors gives rise to the Cristoffel symbols, the numerical evaluation of which may be very inaccurate. Moreover, conservative discrete formulation of the conservation law is no longer straightforward. Some authors derived ''weak-conservative'' formulations in which the Cristoffel symbols are integrated into the fluxes (see, for example, Demirdzic *et al.* [6]). Another interesting approach is due to Karki [13], who avoids the differentiation of the basis vectors by projecting the variables onto a ''local'' cartesian basis, which is related to the curvilinear basis. The Cristoffel symbols do not appear in this formulation but, on the other hand, new metric coefficients which are the inner product of the ''delocalized'' basis vectors arise. Rosenfeld *et al.* [19] obtain similar results by using finite volume techniques and Yang *et al.* [23] generalized this approach.

In the context of $\boldsymbol{v}$–$\boldsymbol{\omega}$ formulation, the work by Pascazio and Napolitano [17] may be quoted. They differentiate the DC problem into a vector Laplace equation which they discretize following the formulation of Rosenfeld *et al.* [19]. In doing this, many metric terms arise and, moreover, the cross-terms are neglected.

We will show that the discretization of the Laplace operator in curvilinear coordinates leads to some difficulties. To overcome these drawbacks, we have developed an algorithm to solve the DC problem in which all metric terms are taken into account and is also fully conservative. This proposed algorithm may be seen as a direct extension of the support-operator concept that was introduced by Favorskii

et al. [7] and that was extended to general elliptic problems by Shashkov and Steinberg [20]. The resulting set of equations is, to some extent, the same as the one that was used by Huang and Ghia [12].

The paper is organized as follows. In the first section we introduce the curvilinear coordinates system and the usual differential first order operators. The DC problem is defined in the second section. This problem will be derived using a so-called "Helmholtz decomposition." Discrete extension of this technique is straightforward, as shown in the third section. The fourth section is devoted to the numerical calculations of some specific problems. We first solve the DC problem with nontrivial curl and divergence over different two-dimensional meshes. Then, we consider the flow with circulation of an inviscid fluid around a two-dimensional circular cylinder, which can be stated as a DC problem. We also solve a three-dimensional DC problem. The application of this technique in the context of the Navier–Stokes equations is illustrated by the computation of the viscous flow around a two-dimensional circular cylinder. The existence and uniqueness of the solution of the discrete DC problem is proven in the appendices.

1. CURVILINEAR COORDINATE SYSTEM

We recall some basic features of tensor analysis. For the sake of simplicity, we adopt tensor notation and the convention of summation over repeated indices. For an introduction to tensor analysis, the reader is referred to the book by Aris [2].

We assume that the computational domain may be described by a general non-orthogonal right-handed curvilinear coordinates system $(\xi^i)_{i=1,2,3}$ and that this mapping is smooth enough so that all definitions make sense. The usual covariant basis vectors are defined by

$$\boldsymbol{e}_j = \frac{\partial \boldsymbol{r}}{\partial \xi^j},$$

where $\boldsymbol{r}$ is the cartesian coordinate vector. They are related to the contravariant basis vectors $\boldsymbol{e}^i$ through the relations

$$\boldsymbol{e}^i \cdot \boldsymbol{e}_j = \delta^i_j,$$

where δ^i_j is the Kronecker symbol. The covariant and contravariant metric tensor are respectively defined by

$$g_{ij} = \boldsymbol{e}_i \cdot \boldsymbol{e}_j, \quad g^{ij} = \boldsymbol{e}^i \cdot \boldsymbol{e}^j.$$

The determinant of the covariant metric tensor is denoted by g. It can be shown [2] that its square root is the Jacobian of the transformation which maps the curvilinear coordinates onto the cartesian ones.

Let $\boldsymbol{v}$ be a vector field which can be expressed as

$$\boldsymbol{v} = v_j \boldsymbol{e}^j = v^i \boldsymbol{e}_i,$$

where v_j ($j = 1, 2, 3$) are the covariant components of the vector $\boldsymbol{v}$ and v^i ($i = 1, 2, 3$) are its contravariant components. This two sets of components are related through the basis transformation chain rules:

$$v_j = g_{ji} v^i, \quad v^i = g^{ij} v_j. \tag{1}$$

Following Yang *et al.* [23], we define the usual vector operators in so-called strong conservative form as follows. The gradient of a scalar field ϕ reads in terms of its covariant components as

$$\nabla \phi = \frac{1}{\sqrt{g}} \frac{\partial \phi}{\partial \xi^j} \boldsymbol{e}^j. \tag{2}$$

The divergence of a vector field $\boldsymbol{v}$ makes use of the contravariant vector components and reads:

$$\nabla \cdot \boldsymbol{v} = \frac{1}{\sqrt{g}} \frac{\partial}{\partial \xi^i} (\sqrt{g} \boldsymbol{v} \cdot \boldsymbol{e}^i). \tag{3}$$

Finally, the curl of $\boldsymbol{v}$ makes use of the covariant vector components and expressed in terms of its contravariant components as

$$\nabla \times \boldsymbol{v} = \frac{1}{\sqrt{g}} \frac{\partial}{\partial \xi^j} (\sqrt{g} \boldsymbol{e}^j \times \boldsymbol{v}). \tag{4}$$

These forms of the first-order differential operators were chosen because their discretization leads to discrete counterpart of the divergence and Stokes theorem.

2. THE DIV-CURL PROBLEM IN CURVILINEAR COORDINATES

This section is devoted to the definition of the DC problem. We show that in the context of curvilinear coordinates, the use of a vector Laplace operator leads to some difficulties and that it seems preferable to perform a Helmholtz decomposition.

2.1. *The Div-Curl Problem*

Let Ω be an open bounded domain, with boundary Γ. It is well known (see Girault and Raviart [10]) that there is a unique vector field $\boldsymbol{v}$ which satisfies

$$\begin{aligned} \nabla \times \boldsymbol{v} &= \boldsymbol{\omega} \quad \text{in } \Omega \\ \nabla \cdot \boldsymbol{v} &= \mathscr{D} \quad \text{in } \Omega \\ \boldsymbol{v} \cdot \boldsymbol{n} &= b \quad \text{on } \Gamma, \end{aligned} \tag{5}$$

where $\boldsymbol{n}$ is the unit outer normal vector to the boundary Γ, $\boldsymbol{\omega}$ is a solenoidal vector field and $\mathscr{D}$ is a scalar function. The scalar data b is defined on the boundary Γ and must satisfy the compatibility constraint,

$$\iint_\Gamma b \, d\Gamma = \iiint_\Omega \mathscr{D} \, d\Omega.$$

In addition, if the domain is p-multiply connected, the circulations c_k of the vector field $\boldsymbol{v}$ on p independent loops γ_k have to be enforced,

$$\int_{\gamma_k} \boldsymbol{v} \cdot \boldsymbol{t} \, dl = c_k, \quad k = 1, ..., p,$$

where $\boldsymbol{t}$ is the unit vector tangent to the loop γ_k and c_k is an arbitrary real constant.

Again, it is assumed that all the functions introduced above are smooth enough; thus precise definitions of functional spaces are not given.

2.2. *The Vector Laplace Operator*

Divergence and curl are first-order operators. The use of second-order operators may appear more convenient for numerical implementation. Differentiating problem (5) and using the well-known vector identity,

$$\nabla^2 \boldsymbol{v} = \nabla(\nabla \cdot \boldsymbol{v}) - \nabla \times \nabla \times \boldsymbol{v}, \tag{6}$$

leads to the equivalent problem:

$$\begin{aligned} \nabla^2 \boldsymbol{v} &= \nabla \mathscr{D} - \nabla \times \boldsymbol{\omega} && \text{in } \Omega \\ (\nabla \times \boldsymbol{v}) \times \boldsymbol{n} &= \boldsymbol{\omega} \times \boldsymbol{n} && \text{on } \Gamma \\ \boldsymbol{v} \cdot \boldsymbol{n} &= b && \text{on } \Gamma. \end{aligned}$$

We refer to Daube [5] for the proof of this result.

Equation (6) highlights an important feature of the vector Laplace operator. Its definition makes use of the divergence operator which acts on the contravariant components *and* of the curl operator which acts on the covariant components. Therefore a choice between covariant and contravariant components has to be made. Whatever this choice is, the contravariant components (resp. covariant) have to be expressed in terms of the covariant (resp. contravariant) components by means of the metric terms, the differentiation of which yields the Cristoffel symbols. This difficulty arises also in the discretization of $\nabla \times \nabla \times \boldsymbol{v}$ since the curl of a covariant vector is a contravariant one.

These remarks suggest solving both covariant and contravariant components. Such a method is proposed in the next section.

2.3. *A New Scheme for the Div-Curl Problem*

The main idea of this algorithm is the use of a Helmholtz-type decomposition. We compute a vector field which has the desired curl and is projected onto the space of divergence-free vectors. This is justified by the following:

PROPOSITION 1. *Let us assume that we know a vector field* $\boldsymbol{w}$ *satisfying*

$$\begin{aligned} \nabla \times \boldsymbol{w} &= \boldsymbol{\omega} \quad && \text{in } \Omega \\ \boldsymbol{w} \cdot \boldsymbol{n} &= b \quad && \text{on } \Gamma \\ \int_{\gamma_k} \boldsymbol{w} \cdot \boldsymbol{t}\, dl &= c_k, \quad && k = 1, ..., p, \end{aligned} \tag{7}$$

and let ϕ *be a solution of*

$$\begin{aligned} \nabla^2 \phi &= \mathscr{D} - \nabla \cdot \boldsymbol{w} \quad && \text{in } \Omega \\ \nabla \phi \cdot \boldsymbol{n} &= 0 \quad && \text{on } \Gamma; \end{aligned}$$

then the vector field $\boldsymbol{v}$ *defined by*

$$\boldsymbol{v} = \boldsymbol{w} + \nabla \phi \tag{8}$$

is the *solution of* (5).

The proof is classical and straightforward.

To summarize, the resolution of the DC problem reduces to two steps:

1. A prediction step which consists in finding *one* vector field which has the desired curl $\boldsymbol{\omega}$.

2. A corrector/projection step which amounts to solving a Poisson problem with Neumann boundary conditions.

Before proceeding with the first step, two remarks have to be made:

• We have seen that the gradient of a scalar function is written in terms of its covariant components (Eq. (2)). It is thus natural to perform the Helmholtz decomposition (8) on the covariant basis.

• The scalar Laplace operator is defined as

$$\nabla^2 \phi = \nabla \cdot (\nabla \phi).$$

Then the divergence operator (3) acts on contravariant components, whereas the gradient (2) is written in terms of covariant components. It is therefore necessary to use the basis transformation chain rules (1). We have to face the same difficulties as others [6, 13, 17] who have dealt with second-order operators in curvilinear coordinates. We will see later that this difficulty can be overcome in our case. We will be able to define two fields that determine the same vector field $\boldsymbol{v}$: one is contravariant and its divergence is $\mathscr{D}$; the second is covariant and its curl is the vorticity $\boldsymbol{\omega}$. Both will be identically connected through the previously mentioned chain rules.

The computation of *one* vector field $\boldsymbol{w}$ (step 1) may be achieved through the resolution of a second-order problem which is obtained by differentiating (7).

PROPOSITION 2. *The problem* (7) *is equivalent to the system:*

$$\begin{aligned} \nabla \times \nabla \times \boldsymbol{w} &= \nabla \times \boldsymbol{v} \quad \text{in } \Omega \\ (\nabla \times \boldsymbol{w}) \times \boldsymbol{n} &= \boldsymbol{\omega} \times \boldsymbol{n} \quad \text{on } \Gamma \\ \boldsymbol{w} \cdot \boldsymbol{n} &= b \quad \text{on } \Gamma. \end{aligned}$$

Proof. Implication is straightforward.

Conversely, lets define the vector field $\boldsymbol{\zeta} = \nabla \times \boldsymbol{w} - \boldsymbol{\omega}$. It is then clear that $\nabla \times \boldsymbol{\zeta} = 0$ in Ω. Furthermore, if $\boldsymbol{\omega}$ is solenoidal, we also have $\nabla \cdot \boldsymbol{\zeta} = 0$ in Ω. Boundary conditions for $\boldsymbol{\zeta}$ on Γ read $\boldsymbol{\zeta} \times \boldsymbol{n} = 0$. We thus get $\boldsymbol{\zeta} = 0$ everywhere, which proves the result. ∎

The Laplace operator has been replaced by the double curl operator $\nabla \times \nabla \times$. Since $\boldsymbol{w}$ is defined by its covariant components, the curl operator may be applied to it, yielding a vector which is defined by its contravariant components. Taking the curl of this last vector therefore necessarily involves Cristoffel symbols, a difficulty which will be overcome in the next section.

3. DISCRETE PROBLEM

Let us assume that the domain Ω can be described by a boundary-fitted system of coordinates (ξ^1, ξ^2, ξ^3) (see Section 1). Without loss of generality it is divided into uniform cells with intervals $\Delta\xi^i = 1$ $(i = 1, 2, 3)$. The center of a *primary* cell corresponds to the indices (l, m, n), the face center by shifting one of these by $\frac{1}{2}$, the edge center by shifting two of these. The primary cells of the inner computational domain are numbered such that $l = 1, ..., L$; $m = 1, ..., M$; and $n = 1, ..., N$. The *secondary* cells are centered on the vertices $(l - \frac{1}{2}, m - \frac{1}{2}, n - \frac{1}{2})$ of the primary grid.

Numerical evaluation of the metric terms requires some attention. We refer to the paper by Rosenfeld *et al.* [19] for a detailed description.

3.1. *Discrete Unknowns and Operators*

In order that the usual vector analysis relations (see further) also hold in the discrete case, we adopt a MAC arrangement for the unknowns (see Harlow and Welch [11]). A scalar field is located at primary cell centers, whereas both covariant (say v_j) and contravariant (say v^i) components of the vector field $\boldsymbol{v}$ are located at primary face centers as sketched in Fig. 1. Here we make use of the fluxes of the vector field across the faces as defined in [19]:

$$v^{(i)} = \sqrt{g} v^i.$$

The transformation chain rules are defined in order to express the contravariant components in terms of the covariant ones. We introduced the linear operator $P^{(i)}$ such that

$$v^{(i)} = P^{(i)}(v_j) \tag{9}$$

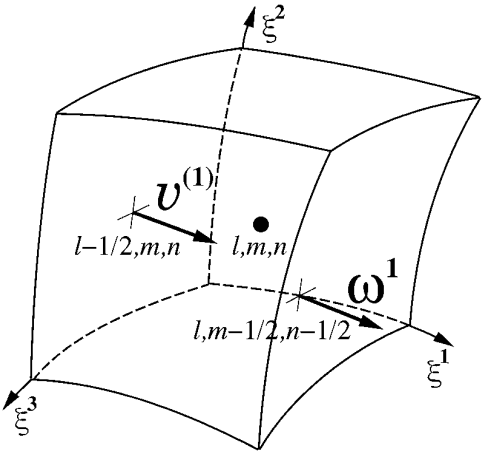

FIG. 1. Definition of a cell and location of the unknowns.

which makes use of the local covariant components v_i and of the neighbouring other covariant components v_{i+1} and v_{i+2} (as illustrated in the two-dimensional case in Fig. 2), multiplied by the discrete metric tensor terms. We propose the operator such that, for instance, the contravariant component along ξ^1 reads

$$\begin{aligned} P^{(1)}(v_j)|_{l-1/2,m,n} = {} & s^{11}v_1|_{l-1/2,m,n} \\ & + \tfrac{1}{4}[s^{12}|_{l,m,n}(v_2|_{l,m-1/2,n} + v_2|_{l,m+1/2,n}) \\ & + s^{12}|_{l-1,m,n}(v_2|_{l-1,m-1/2,n} + v_2|_{l-1,m+1/2,n}) \\ & + s^{13}|_{l,m,n}(v_3|_{l,m,n-1/2} + v_3|_{l,m,n+1/2}) \\ & + s^{13}|_{l-1,m,n}(v_3|_{l-1,m,n-1/2} + v_3|_{l-1,m,n+1/2})], \end{aligned}$$

where $s^{ij} = \sqrt{g}g^{ij}$. This choice is not unique; nevertheless it reduces the storage volume of the metric terms.

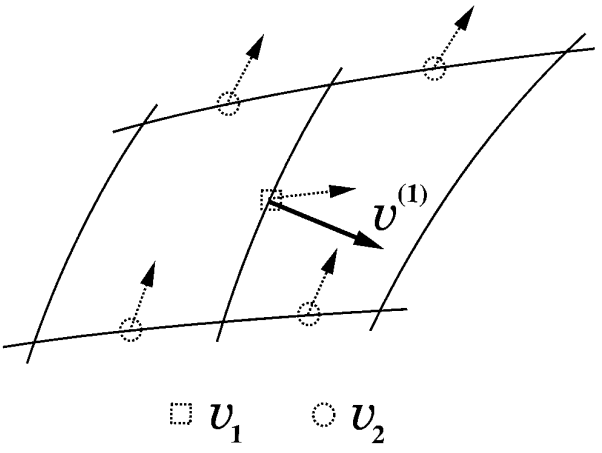

FIG. 2. Definition of the operator $P^{(1)}$ in the 2D case.

The discrete first-order differential operators are obtained by integrating the respective continuous operators along a path, over a surface or in a volume depending on the conservation law for which it is conservative. The gradient (denoted by G^h) of the discrete scalar field ϕ is expressed in terms of the covariant components. For example, the component along ξ^1 reads

$$G^h(\phi)_1|_{l-1/2,m,n} = \phi|_{l,m,n} - \phi|_{l-1,m,n}. \tag{10}$$

The divergence (denoted by D^h) of the discrete vector field $\boldsymbol{v}$ reads

$$\begin{aligned} D^h(v^{(i)})|_{l,m,n} = {} & v^{(1)}|_{l+1/2,m,n} - v^{(1)}|_{l-1/2,m,n} \\ & + v^{(2)}|_{l,m+1/2,n} - v^{(2)}|_{l,m-1/2,n} \\ & + v^{(3)}|_{l,m,n+1/2} - v^{(3)}|_{l,m,n-1/2} \end{aligned} \tag{11}$$

and makes use of the fluxes. The curl (denoted by R^h) of the discrete vector field $\boldsymbol{v}$ is known by its contravariant components located at the primary edge centers, more precisely by its fluxes across the secondary cell surfaces. Its expression makes use of the covariant components of $\boldsymbol{v}$. For example, the component along ξ^3 reads

$$\begin{aligned} R^h(v_j)^{(3)}|_{l-1/2,m-1/2,n} = {} & v_2|_{l,m-1/2,n} - v_2|_{l-1,m-1/2,n} \\ & - v_1|_{l-1/2,m,n} + v_1|_{l-1/2,m-1,n}. \end{aligned} \tag{12}$$

Later on, the upperscript k will denote the contravariant components defined at secondary face centers in order to be distinguished from the contravariant components located at primary face centers, for which the indice i will be preferred.

All these operators are conservative insofar as their summation over adjacent cells identically cancels the intermediate variables. Furthermore, these definitions imply that some well-known vector identities are preserved in the discrete sense. For instance, it is straightforward to show that the (discrete) curl of the (discrete) gradient of any (discrete) scalar field ϕ identically cancels

$$R^h(G^h(\phi)_j)^{(k)} = 0. \tag{13}$$

Let us consider a second divergence operator $\tilde{D}^h$, similar to D^h but defined at the primary cell vertices (i.e., secondary cell centers) and which acts on contravariant components located at the secondary face centers. We then get the (discrete) divergence of the (discrete) curl of any vector field $\boldsymbol{v}$, which is known by its covariant components, and it identically cancels

$$\tilde{D}^h(R^h(v_j)^{(k)}) = 0. \tag{14}$$

Moreover, as stated by Favorskii *et al.* [7], the above definitions ensure that the discrete gradient operator is the transpose of the discrete divergence operator for the bilinear form that is defined as follows. Let us define the inner product of two vectors $\boldsymbol{a}$ and $\boldsymbol{b}$, respectively defined by their covariant and contravariant components, by

$$
\begin{aligned}
(\boldsymbol{a}\cdot\boldsymbol{b})|_{l,m,n} = \tfrac{1}{2}[&(a_1 b^{(1)})|_{l-1/2,m,n} + (a_1 b^{(1)})|_{l+1/2,m,n} \\
&+ (a_2 b^{(2)})|_{l,m-1/2,n} + (a_2 b^{(2)})|_{l,m+1/2,n} \\
&+ (a_3 b^{(3)})|_{l,m,n-1/2} + (a_3 b^{(3)})|_{l,m,n+1/2}].
\end{aligned} \tag{15}
$$

It can then be shown that the discrete analog of the integration by parts of the divergence relationship also holds. Let us multiply the gradient of a scalar field ϕ by the vector field $\boldsymbol{u}$, we get

$$
\begin{aligned}
(G^h(\phi)\cdot\boldsymbol{u})|_{l,m,n} = \tfrac{1}{2}[&(\phi|_{l+1,m,n} - \phi|_{l,m,n})P^{(1)}(u_j)|_{l+1/2,m,n} \\
&+ (\phi|_{l,m,n} - \phi|_{l-1,m,n})P^{(1)}(u_j)|_{l-1/2,m,n} \\
&+ (\phi|_{l,m+1,n} - \phi|_{l,m,n})P^{(2)}(u_j)|_{l,m+1/2,n} \\
&+ (\phi|_{l,m,n} - \phi|_{l,m-1,n})P^{(2)}(u_j)|_{l,m-1/2,n} \\
&+ (\phi|_{l,m,n+1} - \phi|_{l,m,n})P^{(3)}(u_j)|_{l,m,n+1/2} \\
&+ (\phi|_{l,m,n} - \phi|_{l,m,n-1})P^{(3)}(u_j)|_{l,m,n-1/2}].
\end{aligned}
$$

After some algebra, it yields

$$
D^h(\tilde{\phi}P^{(i)}(u_j))|_{l,m,n} = (G^h(\phi)\cdot\boldsymbol{u})|_{l,m,n} + \phi|_{l,m,n} D^h(P^{(i)}(u_j))|_{l,m,n}, \tag{16}
$$

where the new scalar field $\tilde{\phi}$ is defined at the face centers as the half sum of ϕ at the cell centers. This proves the result (see Shashkov and Steinberg [20]).

3.2. *Discrete Equivalence of the DC Problem*

In this section we show that all previously stated results have their own discrete counterpart. In the following we omit the subscripts if not necessary. The discrete version of DC problem (5) takes the form of the following linear system:

$$
\begin{aligned}
R^h(v_j)^{(k)} &= \omega^{(k)} \quad \text{in } \Omega \\
D^h(v^{(i)}) &= \mathscr{D} \quad \text{in } \Omega \\
v^{(p)} &= b^{(p)} \quad \text{on } \Gamma.
\end{aligned} \tag{17}
$$

Here and in the following, the superscript (or subscript) p refers to a component normal to the boundary. The compatibility condition for the boundary scalar field $b^{(p)}$ reads

$$
\begin{aligned}
&\sum_{m=1}^{M}\sum_{n=1}^{N}(b^{(1)}|_{L+1/2,m,n} - b^{(1)}|_{1/2,m,n}) \\
&\quad + \sum_{l=1}^{L}\sum_{n=1}^{N}(b^{(2)}|_{l,M+1/2,n} - b^{(2)}|_{l,1/2,n}) \\
&\quad + \sum_{l=1}^{L}\sum_{m=1}^{M}(b^{(3)}|_{l,m,N+1/2} - b^{(3)}|_{l,m,1/2}) = \sum_{l=1}^{L}\sum_{m=1}^{M}\sum_{n=1}^{N}\mathscr{D}|_{l,m,n}.
\end{aligned} \tag{18}
$$

The contravariant vorticity field $\omega^{(k)}$ must also satisfy the compatibility condition

$$\tilde{D}^h(\omega^{(k)}) = 0$$

in accordance with relation (14).

Both covariant v_j and contravariant $v^{(i)}$ components appear in the linear system (17), which is underdetermined. To complete the system, we need the transformation chain rules (9):

$$v^{(i)} = P^{(i)}(v_j).$$

As mentioned for the continuous case, it is possible to split the discrete covariant components of the vector field $\boldsymbol{v}$ into a rotational and an irrotational part. We get the following.

PROPOSITION 3. *Let us assume that we know the covariant components of a vector field* $\boldsymbol{w}$ *satisfying*

$$\begin{aligned} R^h(w_j)^{(k)} &= \omega^{(k)} \quad \text{in } \Omega \\ w_p &= b_p \quad \text{on } \Gamma, \end{aligned} \tag{19}$$

where the scalar field b_p *is arbitrarily specified on the boundary* Γ, *and let* ϕ *be a* (*discrete*) *scalar function solution of*

$$\begin{aligned} D^h(P^{(i)}(G^h(\phi)_j)) &= \mathscr{D} - D^h(P^{(i)}(w_j)) \quad \text{in } \Omega \\ P^{(p)}(G^h(\phi)_j) &= b^{(p)} - P^{(p)}(w_j) \quad \text{on } \Gamma; \end{aligned} \tag{20}$$

then the vector field $\boldsymbol{v}$ *defined by its covariant components* v_j *such that*

$$v_j = w_j + G^h(\phi)_j \tag{21}$$

is the solution of (17), *where* $v^{(i)} = P^{(i)}(v_j)$.

Proof. Let v_j be the solution of (19), (20), (21). The linearity of operator R^h implies

$$R^h(v_j)^{(k)} = R^h(w_j)^{(k)} + R^h(G^h(\phi)_j)^{(k)}.$$

Because of vector identity (13) the second term of right-hand side cancels and thus $R^h(v_j)^{(k)} = \omega^{(k)}$. In addition the linearity of the operators $P^{(i)}$ and D^h implies

$$D^h(v^{(i)}) = D^h(P^{(i)}(w_j)) + D^h(P^{(i)}(G^h(\phi)_j))$$

and, thus, $D^h(v^{(i)}) = \mathscr{D}$.

Conversely, let $\mathscr{D}'$ be any discrete scalar function, defined at the centers of cells such that

$$\sum_{\Omega} \mathscr{D}' = 0.$$

Since discrete analog of Neumann Poisson equation (20), with $\mathscr{D}'$ as source term, has a unique solution up to an arbitrary constant, it is obvious that the vector component $w_j = v_j - G^h(\phi)_j$ satisfies (19) and $\mathscr{D} = \mathscr{D}' + D^h(P^{(i)}(w_j))$. ▌

The particular case of a multiply-connected domain will be addressed later.

In the proof we assumed that the discrete Neumann Poisson equation has a unique solution. In the context of a curvilinear coordinates system, this was pointed out in the paper of Shashkov and Steinberg [20], but not proven (it is demonstrated here in Appendix B). From the discrete equivalence proposition 3, it is clear that the discrete DC problem (17) has also a unique solution.

It is noteworthy that the first-order differential operators have been defined by integrating the divergence equation over a primary cell volume and integrating the curl over a secondary cell surface. If we then readily define the contravariant component $v^{(i)}$ of the vector field $\boldsymbol{v}$ by its flux across the primary cell surface and its covariant component v_j by its circulation along the secondary cell edge and, also, define $\boldsymbol{\omega}^{(k)}$ and $\mathscr{D}$ as integrals over appropriate surfaces and volumes, respectively, then Eqs. (19) and (20), using definitions (11) and (12), are exact relations, the only numerical approximation being the definition of the linear operator $P^{(i)}$. In principle, that operator can be defined to any order of accuracy.

3.3. *Solving the Prediction Step*

The discrete analog of Proposition 2 makes use of a second curl operator $\tilde{R}^h$ which is defined in a manner similar to that for R^h, except that it acts on the covariant components located at the primary edge centers (i.e., secondary face centers) and that it is defined by means of its contravariant components located at the primary face centers. As mentioned before, differentiating (19) should normally need the projection of the contravariant components of the curl R^h onto the covariant basis. Nevertheless, since the only purpose of the differentiation is to get a second-order problem, the physical meaning of the resultant operator is not a sensitive issue and, therefore, the projection is no longer necessary. Thus, we state

PROPOSITION 4. *Problem* (19) *is equivalent to*

$$\begin{aligned} \tilde{R}^h(R^h(w_j)^{(k)})^{(i)} &= \tilde{R}^h(\boldsymbol{\omega}^{(k)})^{(i)} \quad \text{in } \Omega \\ R^h(w_j)^{(q)} &= \boldsymbol{\omega}^{(q)} \quad \text{on } \Gamma \\ w_p &= b_p \quad \text{on } \Gamma. \end{aligned} \tag{22}$$

Proof. The implication is straightforward.

Conversely let $\boldsymbol{\zeta}$ be the vector field whose contravariant components are $\zeta^{(k)} = R^h(w_j)^{(k)} - \boldsymbol{\omega}^{(k)}$. It satisfies $\tilde{R}^h(\zeta^{(k)})^{(i)} = 0$. Furthermore, since $\boldsymbol{\omega}$ is solenoidal in the sense of $\tilde{D}^h$ and because of relation (14) we get $\tilde{D}^h(\zeta^{(k)}) = 0$. The tangential boundary conditions for $\boldsymbol{\zeta}$ read: $\zeta^{(q)} = 0$. $\boldsymbol{\zeta}$ is therefore the solution of a homogeneous DC problem, whose literal form is the same as in the case of cartesian coordinates. The solution is then $\zeta^{(k)} = 0$ everywhere. ▌

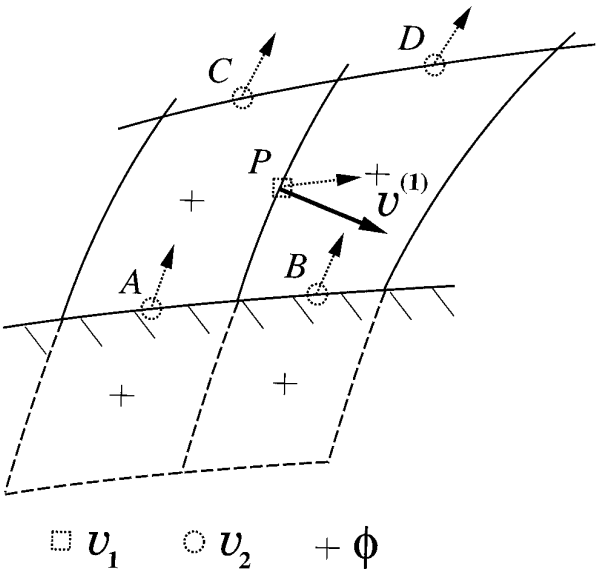

FIG. 3. Definition of the operator $P^{(1)}$ near the boundary in the 2D case.

We note that the scalar field b_p is not part of the initial discrete DC problem (17). Its value can therefore be chosen arbitrarily, but it is needed in order to define the curl of $\boldsymbol{w}$ on the boundaries (relation (12)). Nevertheless, it seems natural to define it as

$$b_p = \boldsymbol{b} \cdot \boldsymbol{e}_p$$

where $\boldsymbol{b}$ is a vector field such that $b^{(p)} = \boldsymbol{b} \cdot \boldsymbol{e}^{(p)}$.

The second-order double curl operator is parabolized with respect to a pseudo-time τ in order to be solved iteratively. The algorithm reads

$$\frac{\partial w_j}{\partial \tau} + \tilde{R}^h(R^h(w_j)^{(k)})^{(i)} = \tilde{R}^h(\omega^{(k)})^{(i)} \quad \text{in } \Omega$$

$$R^h(w_j)^{(q)} = \omega^{(q)} \quad \text{on } \Gamma.$$

This algorithm is proven to be unconditionally stable (Appendix A).

3.4. *Boundary Conditions*

As outlined by Bernard and Kapitza [3] some difficulties arise with the boundary conditions. Recall that the discretization of the Laplace operator (20) involves the contravariant components of the gradient. Let us consider a cell adjacent to the boundary as sketched in Fig. 3. The contravariant component at point P is computed by linear interpolation over the covariant components at the points P, A, B, C, and D. The difficulty lies in the fact that the evaluation of the covariant component of the gradient $G^h(\phi)_2$ at points A and B requires the value of ϕ at the center of a

fictitious cell outside the computational grid. To overcome this difficulty Bernard and Kapitza make use of a linear extrapolation in order to calculate this value.

We propose a different approach. Actually the Dirichlet condition on the covariant component

$$w_p = b_p,$$

which was introduced in (19), has to be preserved after the projection step, thus yielding

$$v_p = b_p.$$

Introducing the Helmholtz decompostion (21), we get a Neumann-type boundary condition for the scalar field ϕ:

$$G^h(\phi)_p = 0.$$

The values of ϕ outside the grid are then set equal to their values at the center of the cell adjacent to the boundary.

As a result, we are here able to control the projection of the solution vector field onto the covariant basis ''normal'' to the boundary, whereas in the work by Bernard and Kapitza this projection depends on the extrapolation procedure.

3.5. *Multiply-Connected Domain*

Let us now consider the case of a p-multiply connected domain. As mentioned before it is required to enforce the circulation of the vector field $\boldsymbol{v}$ on p independent loop γ_k, in order to ensure the uniqueness of the solution.

In the context of a Helmholtz decomposition, it is obvious that if the vector field $\boldsymbol{w}$ has the desired circulation, it is also true for the vector field $\boldsymbol{v}$ since the circulation of the (discrete) gradient cancels along any loop.

Enforcing the circulation of the vector field $\boldsymbol{w}$ is an easy task. Let us assume that we found a vector field $\boldsymbol{w}'$ that satisfies the curl relation (19) and let us denote c'_k as its circulation:

$$\int_{\gamma_k} \boldsymbol{w}' \cdot \boldsymbol{t}\, dl = c'_k.$$

Let us now define the discrete vector field $\boldsymbol{x}$ by its covariant components x_j such that

- $x_j = c_k - c'_k$ on one arbitrary plane (a line in 2D) $\xi^j = \text{const}$ starting from the obstacle Γ_k and intersecting the path γ_k.
- $x_j = 0$, otherwise.
- the two components x_{j+1} and x_{j+2} are 0 everywhere.

The discrete curl of $\boldsymbol{x}$ obviously cancels and its circulation along γ_k is $c_k - c'_k$. Let the vector field $\boldsymbol{w}$ be defined such that

$$w_j = w'_j + x_j;$$

then its curl and circulation have the desired values.

4. NUMERICAL TESTS

In order to test and validate the above-described algorithm, we have performed calculations over several meshes as defined by Shashkov and Steinberg [20]. These authors solved elliptic problems for a scalar function, but also interpreted the results for the fluxes of the quantity. The contravariant component of a vector field being analogous to those fluxes, we expect similar results. In order to analyse these computations, we need to define some error norms. For further details on truncation error analysis and definition of the order of accuracy of finite-difference schemes, the reader is referred to the book by Strikwerda [22] or the paper by Knorr *et al.* [14].

Along the line of [20], let us define the two invariant norms as follows. Let the discrete vector field $\boldsymbol{v}$ be given by its flux contravariant components $(v^{(1)}, v^{(2)})$ defined at the face centers and introduce the cell-centered vector field $\tilde{\boldsymbol{v}}$ such that

$$\tilde{\boldsymbol{v}}|_{l,m} = (\tilde{v}^1, \tilde{v}^2) = \frac{1}{\sqrt{g}|_{l,m}} \left(\frac{v^{(1)}|_{l,m} + v^{(1)}|_{l+1,m}}{2}, \frac{v^{(2)}|_{l,m} + v^{(2)}|_{l,m+1}}{2} \right);$$

then the max and the l_2 norms are defined by

$$\|\boldsymbol{v}\|_\infty = \max_l \max_m (\max(|\tilde{v}^1|_{l,m}|, |\tilde{v}^2|_{l,m}|))$$

$$\|\boldsymbol{v}\|_2^2 = \sum_{l=1}^{L} \sum_{m=1}^{M} \sqrt{g}|_{l,m} ((\tilde{v}^1|_{l,m})^2 + (\tilde{v}^2|_{l,m})^2).$$

Let $\boldsymbol{u}$ be the exact solution of the problem (17) and let $\boldsymbol{v}$ be the approximate solution. The errors corresponding to the two norms are given by

$$E_\infty(\boldsymbol{v}) = \|\boldsymbol{u} - \boldsymbol{v}\|_\infty$$

$$E_2(\boldsymbol{v}) = \|\boldsymbol{u} - \boldsymbol{v}\|_2.$$

In order to compare the results for the scalar function to those of [20], we also define the following norms for the scalar function ϕ:

$$\|\phi\|_\infty = \max_l \max_m (|\phi|_{l,m}|)$$

$$\|\phi\|_2^2 = \sum_{l=1}^{L} \sum_{m=1}^{M} \sqrt{g}|_{l,m} (\phi|_{l,m})^2.$$

In the numerical tests the number of cells in the two directions is identical and equal to $L = M = 2^r$. Then the mesh size h is proportional to $h = 2^{-r}$. The two norms of errors are expected to verify $E(r) \approx Ch^k$, where C and k are constant if h is sufficiently small. The order k of the error is then defined by

$$k = \lim_{r\to\infty} \log_2 \frac{E(r)}{E(r+1)}.$$

Once k have been determined, the error constant can be computed as

$$C = \lim_{r\to\infty} 2^{kr} E(r).$$

In the following we perform two classes of tests. We first solved the DC problem over meshes defined in [20]. Then we consider the problem over a doubly-connected domain and solve the problem of the flow of an inviscid fluid with circulation around a circular cylinder.

4.1. *Two-Dimensional DC Problem on Simply-Connected Domains*

Several grids are defined to perform our calculations. They are the same as those used by Shashkov and Steinberg [20]. The first is the mapping of the unit square,

$$x = \xi + \varepsilon\xi(1-\xi)(\tfrac{1}{2}-\xi)\eta(1-\eta)$$
$$y = \eta + \varepsilon\eta(1-\eta)(\tfrac{1}{2}-\eta)\xi(1-\xi),$$

where ξ and η vary between 0 and 1 with the indices l and m such that $\xi = l/(L+1)$ and $\eta = m/(M+1)$. The coefficient ε is a measure of departure from orthogonality.

The second class of mappings is elliptical,

$$x = r\cos(\theta), \quad y = ar\sin(\theta),$$

where:

$$r = 1 + \xi, \quad \theta = \pi\eta/2.$$

The general grid transformation is defined by

$$x = \xi + \varepsilon\cos\left(\frac{\pi}{4}(\xi+\eta)\right),$$
$$y = \eta + \varepsilon\sin\left(\frac{\pi}{4}(\xi+\eta)\right).$$

The exact solution is chosen in accordance with [20] for all the calculations. The cartesian vector field reads

$$\boldsymbol{u}(x, y) = \boldsymbol{K}\cdot\nabla(\varphi),$$

where the scalar function φ is given by

TABLE I
Square with $\varepsilon = 0$

N order	Max order	Mean order	Max constant 2	Mean constant 2	Max order	Mean order	Max constant 3	Mean constant 3
8			1.77	1.07			2.04	1.62
16	2.01	2.01	1.76	1.06	2.97	2.99	2.08	1.63
32	2.00	2.00	1.75	1.06	2.99	3.00	2.09	1.63
64	2.00	2.00	1.75	1.06	3.00	3.00	2.09	1.64
128	2.00	2.00	1.75	1.06	3.00	3.00	2.09	1.64
256	2.00	2.00	1.76	1.06	3.00	3.00	2.09	1.64
[20]	2.0	2.0	0.92	0.57	0.88	1.6	0.22	0.21

$$\varphi = \sin(\pi x)\,\sin(\pi y).$$

The matrix $\boldsymbol{K}$ is the rotation of angle $3\pi/12$ of the diagonal matrix,

$$\boldsymbol{D} = \mathrm{diag}(d_1, d_2) \quad \text{with } d_1 = 1 + 2x^2 + y^2,\ d_2 = 1 + x^2 + 2y^2.$$

Boundary conditions are given by the same vector field. Note that general mixed boundary conditions were used in [20] for the general elliptic problem. In our case, it reduces to Neumann conditions.

As outlined before, we also compare the results for the scalar function. To do this, we first fit our calculation with the discrete vorticity of the exact solution $\boldsymbol{u}$. The consequence is that the error of the approximate solution $\boldsymbol{v}$ writes in the form of a gradient:

$$\boldsymbol{u} - \boldsymbol{v} = \nabla(\phi).$$

Then this gradient should cancel when the approximate field converges to the exact field, or ϕ should be a constant. Since $\boldsymbol{v}$ has been calculated, we integrate the gradient in order to obtain ϕ. The difference between ϕ and its average value is an estimate of the scalar error of the scheme. The linear equations are solved until convergence is reached.

Results are reported in the tables. The first column gives the number of points in the grid. The next four columns give the data for the scalar error, while the last four columns give the data for the fluxes. Table I gives the results for the uniform grid (square with $\varepsilon = 0$), whereas Table II gives the data for the nonorthogonal mapping of the square with $\varepsilon = 10$. Tables III and IV give the data for elliptical grids with $a = 1$ and $a = 2$ respectively, and Tables V and VI for the general nonorthogonal grid with $\varepsilon = 0.25$ and $\varepsilon = 0.5$. In those tables are also reported the results of Shashkov and Steinberg [20] for the finest grid (i.e., $L = M = 256$).

We observe that in our case, the order of accuracy always converges to two for the scalar norm as found by [20], but between two and three for the fluxes norm, whereas [20] always found an order lower than two. Constants are of the same

TABLE II
Square with $\varepsilon = 10$

N	Max order	Mean order	Max constant 2	Mean constant 2	Max order	Mean order	Max constant 1.8	Mean constant 2.6
8			10.09	4.14			1.85	7.05
16	1.51	1.73	14.15	4.99	2.84	2.92	0.90	5.65
32	1.72	1.73	17.18	6.03	2.55	2.87	0.54	4.69
64	1.88	1.83	18.71	6.76	1.80	2.71	0.53	4.35
128	1.94	1.91	19.50	7.18	1.74	2.61	0.56	4.31
256	1.97	1.96	19.87	7.40	1.83	2.56	0.55	4.42
[20]	2.0	2.0	6.5	3.2	1.00	1.5	2.6	2.6

TABLE III
Elliptical with $a = 1$

N	Max order	Mean order	Max constant 2	Mean constant 2	Max order	Mean order	Max constant 3	Mean constant 3
8			15.58	11.08			66.	52.8
16	1.89	2.11	16.76	10.24	2.32	2.75	106.	62.6
32	2.01	2.03	16.65	10.06	2.82	2.94	120.	65.5
64	2.00	2.01	16.44	10.02	2.96	2.98	123.	66.2
128	2.00	2.00	16.47	10.01	2.99	3.00	124.	66.4
256	2.00	2.00	16.46	10.01	3.00	3.00	124.	66.4
[20]	2.0	2.0	1.4	0.58	1.0	1.8	0.64	2.1

TABLE IV
Elliptical with $a = 2$

N	Max order	Mean order	Max constant 1.96	Mean constant 2	Max order	Mean order	Max constant 2.9	Mean constant 3
8			165.	132.			1078.	1130.
16	1.70	1.84	197.	148.	2.05	2.55	1946.	1545.
32	1.48	1.85	274.	164.	2.50	2.80	2565.	1773.
64	1.82	1.93	303.	172.	2.83	2.94	2696.	1854.
128	1.96	1.99	310.	175.	2.91	2.98	2672.	1882.
256	1.96	1.99	309.	176.	2.93	2.99	2623.	1892.
[20]	2.0	2.0	20.	14.	0.65	1.9	22.	330.

TABLE V
General Transformation with $\varepsilon = 0.25$

N order	Max order	Mean order	Max constant 2	Mean constant 2	Max order	Mean order	Max constant 2.4	Mean constant 3
8			1.22	0.65			0.80	1.54
16	2.23	2.31	1.04	0.53	2.92	2.99	0.56	1.55
32	2.13	2.16	0.96	0.47	2.87	2.99	0.40	1.57
64	2.07	2.08	0.91	0.45	2.75	3.00	0.31	1.56
128	2.04	2.04	0.89	0.44	2.59	2.99	0.27	1.57
256	2.02	2.02	0.88	0.43	2.42	2.98	0.27	1.59
[20]	2.0	2.0	1.1	0.58	0.87	1.7	0.31	1.3

order of those found by Shashkov *et al.* [20], except for the elliptical grids where they are found to be higher. A possible explanation of these discrepancies might be that the boundary conditions slightly differ. In particular, the use of Neumann boundary conditions instead of general mixed ones may be the reason for better performance in our computation of the fluxes.

4.2. *Doubly-Connected Domain*

We check the ability of the methodology to deal with nonsimply connected domain by computing the irrotationnal inviscid flow with circulation around a two-dimensional circular cylinder. Let C_0 be the circulation around the cylinder, and define the complex velocity

$$u - iv = V_0 - V_0 \frac{R^2}{Z^2} + \frac{iC_0}{2\pi Z}, \tag{23}$$

where u and v are the cartesian velocity components, V_0 is the velocity at infinity,

TABLE VI
General Transformation with $\varepsilon = 0.5$

N order	Max order	Mean order	Max constant 2	Mean constant 2	Max order	Mean order	Max constant 2.2	Mean constant 2.9
8			2.21	1.06			1.28	2.78
16	1.97	2.00	2.26	1.06	2.70	2.82	0.91	2.93
32	1.67	1.80	2.85	1.22	2.70	2.92	0.64	2.89
64	1.85	1.84	3.17	1.36	2.59	2.95	0.49	2.79
128	1.92	1.90	3.35	1.46	2.44	2.95	0.41	2.69
256	1.96	1.94	3.46	1.52	2.24	2.93	0.40	2.64
[20]	2.0	2.0	1.4	0.58	1.0	1.8	0.64	2.1

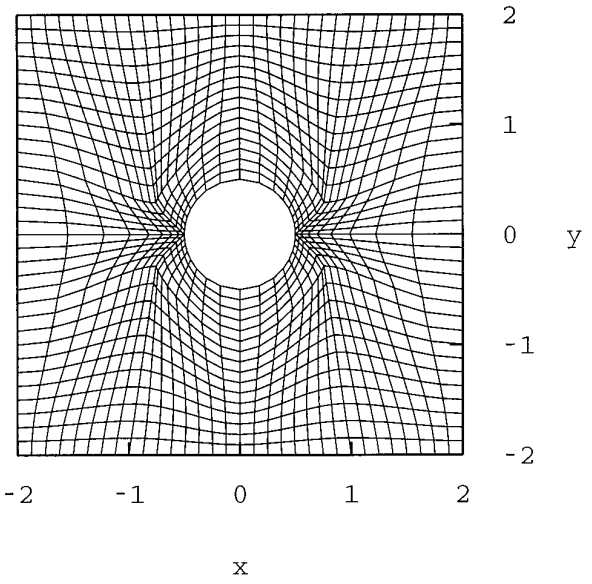

FIG. 4. H-mesh around the cylinder (1 mesh-line over 4).

R the radius of the cylinder, $Z = x + iy$ the complex variable. Then u and v are the exact solution of the problem (17) with $\omega = 0$ and boundary conditions given by (23). The H-type mesh of the domain, which extend over three diameters around the cylinder is presented in Fig. 4. The mesh has been refined near the singularity in order to increase the accuracy. The configuration of the calculation is chosen as

$$V_0 = 1, \quad R = \frac{1}{2}, C_0 = 4.$$

The streamlines are presented in Fig. 5 for the exact solution, and in Fig. 6 for the approximate solution. They are in good agreement.

4.3. *Three-Dimensional DC Problem*

The calculation of the DC problem in the three-dimensional case is achieved in the same spirit as for the two-dimensional one. The grid used is the mapping of the unit square defined by

$$\begin{aligned} x &= \xi + \varepsilon\xi(1-\xi)(\tfrac{1}{2}-\xi)\eta(1-\eta)\zeta(1-\zeta) \\ y &= \eta + \varepsilon\eta(1-\eta)(\tfrac{1}{2}-\eta)\xi(1-\xi)\zeta(1-\zeta) \\ z &= \zeta + \varepsilon\zeta(1-\zeta)(\tfrac{1}{2}-\zeta)\xi(1-\xi)\eta(1-\eta). \end{aligned}$$

The exact solution reads

$$\boldsymbol{u}(x, y, z) = \boldsymbol{K}\cdot\nabla(\varphi),$$

where the scalar function φ is given by

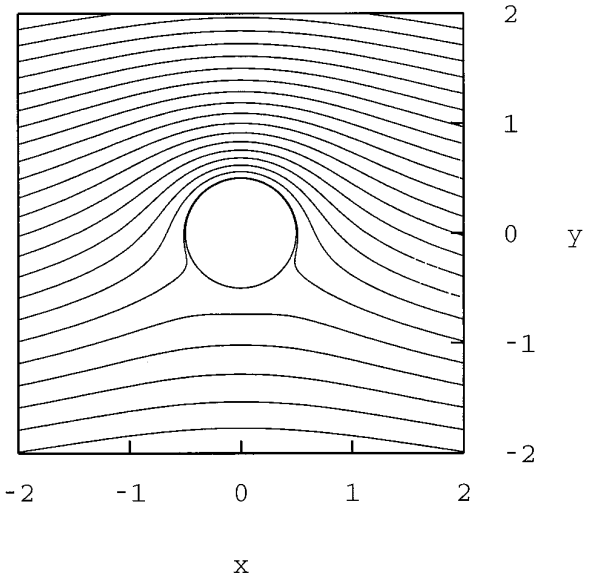

FIG. 5. Streamlines around the cylinder—exact solution.

$$\varphi = \sin(\pi x)\,\sin(\pi y)\,\sin(\pi z).$$

The matrix $\boldsymbol{K}$ is the combination of the rotations of angle $3\pi/12$ around the z-axis and around the y-axis of the diagonal matrix defined by

$$\boldsymbol{D} = \mathrm{diag}(d_1, d_2, d_3)$$

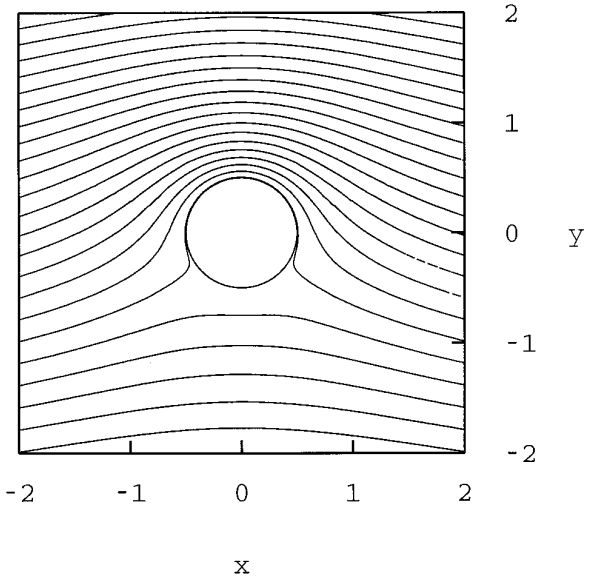

FIG. 6. Streamlines around the cylinder—approximate solution.

TABLE VII
Three-Dimensional Square with $\varepsilon = 0$

N order	Max order	Mean order	Max constant 2	Mean constant 2	Max order	Mean order	Max constant 3.5	Mean constant 3.5
8			1.71	1.07			1.71	1.40
16	2.02	2.02	1.69	1.05	3.48	3.49	1.74	1.41
32	2.01	2.00	1.68	1.05	3.49	3.50	1.74	1.42
64	2.00	2.00	1.68	1.05	3.50	3.50	1.74	1.42

with

$$d_1 = 1 + 2x^2 + y^2 + z^2, \quad d_2 = 1 + x^2 + 2y^2 + z^2, \quad d_3 = 1 + x^2 + y^2 + 2z^2.$$

Results are reported in Table VII for $\varepsilon = 0$ and Table VIII for $\varepsilon = 10$. They are very like the two-dimensional case for the scalar errors. The errors for the fluxes are better for both the orthogonal and the nonorthogonal cases.

4.4. *Viscous Flow around a Circular Cylinder*

Despite the fact that the resolution of the Navier–Stokes equations is beyond the scope of this paper, we illustrate the use of our method by solving these equations under velocity–vorticity formulation (see the Introduction). Further details on the resolution can be found in [4].

We compute the two-dimensional flow of an incompressible viscous fluid around a circular cylinder. The Reynolds number based on the cylinder diameter and the velocity at infinity is Re = 100. We use a H-type grid which is strongly nonorthogonal. In order to test the method, the flowfield has an incidence of 45° relative to this mesh. Figure 7 shows a partial view of the grid around the cylinder, whereas Figs. 8 and 9 show the streamlines and the dynamic pressure isovalues at time $t = 2$. The symmetry of the results proves the efficiency of the method on such grids.

TABLE VIII
Three-Dimensional Square with $\varepsilon = 10$

N order	Max order	Mean order	Max constant 2	Mean constant 2	Max order	Mean order	Max constant 2.2	Mean constant 3.2
8			3.07	1.06			0.15	0.89
16	1.95	1.99	3.18	1.07	3.21	3.44	0.07	0.76
32	1.99	2.00	3.19	1.07	2.71	3.33	0.05	0.70
64	2.00	2.00	3.19	1.07	2.24	3.18	0.05	0.71

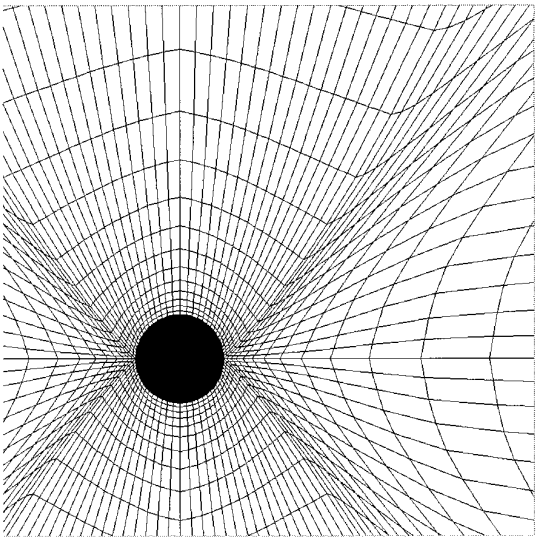

FIG. 7. Grid around the circular cylinder (1 mesh-line over 2).

CONCLUSION

We proposed a new method for solving the DC problem which naturally extends to general curvilinear coordinates by using a Helmholtz-type decomposition of the solution vector field. Both covariant and contravariant components have to be considered so that the divergence and the curl of the vector field are satisfied to within the machine accuracy.

The implementation of a projection operator expressing the contravariant compo-

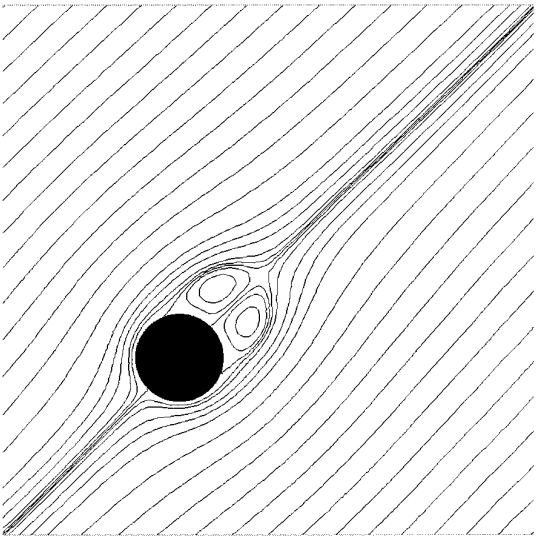

FIG. 8. Streamlines of the viscous flow around a circular cylinder.

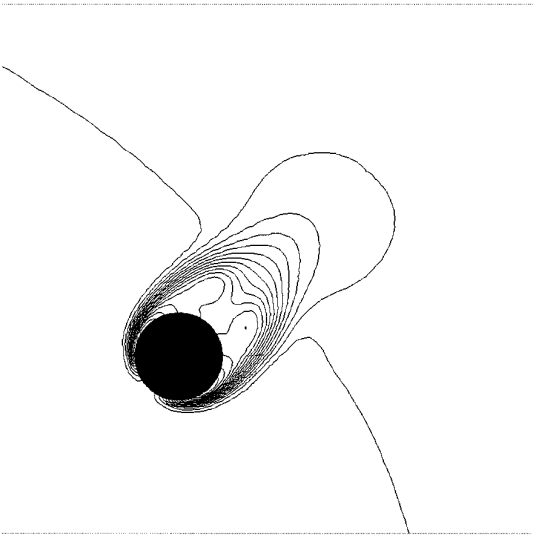

FIG. 9. Isovalues of the dynamic pressure around a circular cylinder.

nents in terms of the covariant ones is an important feature of this technique. Furthermore, this integral formulation of the DC problem can in principle be applied to a general unstructured grid and its dual. As mentioned in the introduction, the DC problem has already been treated by several authors (e.g., [1, 15]) when these meshes are orthogonal to one another. Thus, making use of such a projection operator would be a solution for dealing with more general meshes.

This technique can be used to solve the kinematical problem of the Navier–Stokes equations in velocity–vorticity form. In this context, the flow around a circular cylinder has been successfully computed.

APPENDIXES

A. *Convergence of the Curl-Curl Algorithm*

We prove the convergence of the algorithm only in the two-dimensional case. A similar demonstration could be drawn up in three dimensions.

We have to solve the following algorithm for the vector field $\boldsymbol{w}$ which is split into its two components $\boldsymbol{w} = (u, v)$:

$$\frac{\partial u^{n+1}}{\partial \tau} - \frac{\partial^2 u^{n+1}}{\partial y^2} + \frac{\partial}{\partial y}\frac{\partial v^n}{\partial x} = + \frac{\partial \omega}{\partial y}$$

$$\frac{\partial v^{n+1}}{\partial \tau} + \frac{\partial}{\partial x}\frac{\partial u^{n+1}}{\partial y} - \frac{\partial^2 v^{n+1}}{\partial x^2} = - \frac{\partial \omega}{\partial x}.$$

Let δ_{xx} be the classical second-order approximation of the one-dimensional second derivative on an uniform grid containing M grid points. We will denote by $(\boldsymbol{f}^k_M$,

α_M^k) the eigenelements of δ_{xx} fitted with Dirichlet boundary conditions, and by ($\boldsymbol{e}_M^k$, β_M^k) the eigenelements of δ_{xx} fitted with Neumann boundary conditions. They read

$$\boldsymbol{f}_M^k|_j = \sin\left(j\,\frac{k\pi}{M}\right)_{(j=0,M)}$$

$$\alpha_M^k = -4\sin^2\left(\frac{k\pi}{2M}\right)$$

for $k = 1$ to $M - 1$, and

$$\boldsymbol{e}_M^k|_j = \cos\left(\left(j - \frac{1}{2}\right)\frac{k\pi}{M}\right)_{(j=0,M)}$$

$$\beta_M^k = -4\sin^2\left(\frac{k\pi}{2M}\right)$$

for $k = 0$ to $M - 1$. It is a simple matter to show that

$$\delta_x(\boldsymbol{f}_M^k) = +2\sin\left(\frac{k\pi}{2M}\right)\boldsymbol{e}_M^k$$

and

$$\delta_x(\boldsymbol{e}_M^k) = -2\sin\left(\frac{k\pi}{2M}\right)\boldsymbol{f}_M^k,$$

where δ_x denotes the classical approximation of the first-order derivative.

Both components of the vector field can be projected on these basis using tensor convention,

$$u = \hat{u}_{ij}\boldsymbol{f}_L^i \otimes \boldsymbol{e}_M^j$$
$$v = \hat{v}_{ij}\boldsymbol{e}_L^i \otimes \boldsymbol{f}_M^j,$$

and the vorticity,

$$\omega = \hat{\omega}_{ij}\boldsymbol{f}_L^i \otimes \boldsymbol{f}_M^j.$$

Hence, the algorithm reads on the tensorial basis,

$$\frac{\hat{u}_{ij}^{n+1} - \hat{u}_{ij}^{n}}{\Delta\tau} + \mu_j^2 \hat{u}_{ij}^{n+1} - \lambda_i \mu_j \hat{v}_{ij}^{n} = + \mu_j \hat{\omega}_{ij} \quad \text{(with respect to } \boldsymbol{f}_L^i \otimes \boldsymbol{e}_M^j\text{)}$$

$$\frac{\hat{v}_{ij}^{n+1} - \hat{v}_{ij}^{n}}{\Delta\tau} - \lambda_i \mu_j \hat{u}_{ij}^{n+1} + \lambda_i^2 \hat{v}_{ij}^{n+1} = - \lambda_i \hat{\omega}_{ij} \quad \text{(with respect to } \boldsymbol{e}_L^i \otimes \boldsymbol{f}_M^j\text{)},$$

where

$$\lambda_i = 2 \sin\left(\frac{i\pi}{2L}\right), \quad \mu_j = 2 \sin\left(\frac{j\pi}{2M}\right).$$

In matrix form we get

$$\begin{pmatrix} 1 + \Delta\tau\mu_j^2 & 0 \\ -\Delta\tau\lambda_i\mu_j & 1 + \Delta\tau\,\lambda_i^2 \end{pmatrix} \begin{pmatrix} \hat{u}_{ij}^{n+1} \\ \hat{v}_{ij}^{n+1} \end{pmatrix} = \begin{pmatrix} 1 & +\Delta\tau\lambda_i\mu_j \\ 0 & 1 \end{pmatrix} \begin{pmatrix} \hat{u}_{ij}^{n} \\ \hat{v}_{ij}^{n} \end{pmatrix} + \begin{pmatrix} +\mu_j\hat{\omega}_{ij} \\ -\lambda_i\hat{\omega}_{ij} \end{pmatrix}.$$

Therefore, the resolution of each mode is independent of the other ones. Define λ and μ as

$$\lambda = \sqrt{\Delta\tau}\lambda_i, \quad \mu = \sqrt{\Delta\tau}\mu_j.$$

Multiplying by the inverse matrix in the left hand side, it yields

$$\begin{pmatrix} \hat{u}^{n+1} \\ \hat{v}^{n+1} \end{pmatrix} = \frac{1}{(1+\lambda^2)(1+\mu^2)} \left[\begin{pmatrix} 1 + \lambda^2 & \lambda\mu(1+\lambda^2) \\ \lambda\mu & (\lambda\mu)^2 + (1+\mu^2) \end{pmatrix} \begin{pmatrix} \hat{u}^{n} \\ \hat{v}^{n} \end{pmatrix} + \begin{pmatrix} \mu(1+\lambda^2)\hat{\omega} \\ [\mu(\lambda\mu) - \lambda(1+\mu^2)]\hat{\omega} \end{pmatrix} \right].$$

This system is now expressed in the eigenbasis of the matrix in the right-hand side. Lets define the basis transformation as

$$\begin{pmatrix} \hat{u} \\ \hat{v} \end{pmatrix} = \begin{pmatrix} \lambda & \mu(1+\lambda^2) \\ \mu & -\lambda \end{pmatrix} \begin{pmatrix} \tilde{u} \\ \tilde{v} \end{pmatrix}.$$

The system thus reads

$$\begin{pmatrix} \tilde{u}^{n+1} \\ \tilde{v}^{n+1} \end{pmatrix} = \begin{pmatrix} 1 & 0 \\ 0 & \dfrac{1}{(1+\lambda^2)(1+\mu^2)} \end{pmatrix} \begin{pmatrix} \tilde{u}^{n} \\ \tilde{v}^{n} \end{pmatrix} + \begin{pmatrix} 0 \\ \dfrac{\hat{\omega}}{(1+\lambda^2)(1+\mu^2)} \end{pmatrix}.$$

It is then obvious that this algorithm converges towards a steady state independently of the pseudo-time step $\Delta\tau$. Furthermore, the larger this pseudo-time step is, the

lower is the amplification factor of the matrix and the higher is the rate of convergence of the algorithm.

B. *Existence and Uniqueness of Solution of the Poisson Equation*

It is well known that there exists a unique solution of the Laplace equation with Neumann boundary conditions in the context of orthogonal grids. In this section it is shown that the solution of (20) exists and is unique for general curvilinear coordinate systems under some particular geometric conditions. For the sake of simplicity we only consider the two-dimensional homogeneous problem; similar results could be obtained in the three-dimensional case.

B.1. *Homogeneous Poisson equation.* The homogeneous problem reads

$$D^h(P^{(i)}(G^h(\phi)_j)) = 0 \tag{B.1}$$

$$P^{(p)}(G^h(\phi)_j) = 0, \tag{B.2}$$

where the linear operators D^h, G^h, and $P^{(i)}$ are respectively the divergence, the gradient, and the projection from the covariant to the contravariant components, in the discrete sense. The existence of solution is straightforward. Indeed, the compatibility condition is obviously satisfied and we know that any linear operator in finite dimension is surjective. Let us now prove the uniqueness of the solution.

B.2. *Unicity.* Proving the uniqueness of the solution is equivalent to proving that the operator associated with the Poisson equation with boundary conditions is injective.

Let us multiply Eq. (B.1) by ϕ. Making use of the discrete integration by part (16), we get

$$D^h(\tilde{\phi}P^{(i)}(G^h(\phi)_j)) - (G^h(\phi) \cdot G^h(\phi)) = 0,$$

where the scalar field $\tilde{\phi}$ located at face centers is defined as the half sum of the scalar field ϕ at adjacent cell centers, and the inner product of the gradient of ϕ with itself is defined by (15), where $G^h(\phi)^{(i)} = P^{(i)}(G^h(\phi)_j)$.

Let us now sum this last equation over the whole computational domain Ω. The conservative form of the divergence operator yields the values of the homogeneous Neumann boundary condition on the boundary. We get

$$\sum_{\Omega} (G^h(\phi) \cdot G^h(\phi)) = 0.$$

The uniqueness of the solution now reduces to prove that the bilinear form,

$$(\boldsymbol{u}, \boldsymbol{v}) = \sum_{\Omega} (\boldsymbol{u} \cdot \boldsymbol{v}),$$

is positive and definite. Let us explicitly write this form:

$$
\begin{aligned}
(\boldsymbol{u},\boldsymbol{v}) = \frac{1}{2}\sum_{\Omega}\Bigg[& u_1|_{l-1/2,m}\left(s^{11}|_{l-1/2,m}v_1|_{l-1/2,m} + \frac{1}{4}\left(s^{12}|_{l,m}(v_2|_{l,m-1/2} + v_2|_{l,m+1/2})\right.\right.\\
& \left.\left. + s^{12}|_{l-1,m}(v_2|_{l-1,m-1/2} + v_2|_{l-1,m+1/2})\right)\right)\\
& + u_1|_{l+1/2,m}\left(s^{11}|_{l+1/2,m}v_1|_{l+1/2,m} + \frac{1}{4}\left(s^{12}|_{l,m}(v_2|_{l,m-1/2} + v_2|_{l,m+1/2})\right.\right.\\
& \left.\left. + s^{12}|_{l+1,m}(v_2|_{l+1,m-1/2} + v_2|_{l+1,m+1/2})\right)\right)\\
& + u_2|_{l,m-1/2}\left(s^{22}|_{l,m-1/2}v_2|_{l,m-1/2} + \frac{1}{4}\left(s^{12}|_{l,m}(v_1|_{l-1/2,m} + v_1|_{l+1/2,m})\right.\right.\\
& \left.\left. + s^{12}|_{l,m-1}(v_1|_{l-1/2,m-1} + v_1|_{l+1/2,m-1})\right)\right)\\
& + u_2|_{l,m+1/2}\left(s^{22}|_{l,m+1/2}v_2|_{l,m+1/2} + \frac{1}{4}\left(s^{12}|_{l,m}(v_1|_{l-1/2,m} + v_1|_{l+1/2,m})\right.\right.\\
& \left.\left. + s^{12}|_{l,m+1}(v_1|_{l-1/2,m+1} + v_1|_{l+1/2,m+1})\right)\right)\Bigg].
\end{aligned}
$$

Rearranging this sum by incorporating the terms of adjacent cells we get

$$
\begin{aligned}
(\boldsymbol{u},\boldsymbol{v}) = \frac{1}{2}\sum_{\Omega}\Bigg[& u_1|_{l-1/2,m}\left(s^{11}|_{l-1/2,m}v_1|_{l-1/2,m} + \frac{1}{2}\left(s^{12}|_{l,m}(v_2|_{l,m-1/2} + v_2|_{l,m+1/2})\right)\right)\\
& + u_1|_{l+1/2,m}\left(s^{11}|_{l+1/2,m}v_1|_{l+1/2,m} + \frac{1}{2}\left(s^{12}|_{l,m}(v_2|_{l,m-1/2} + v_2|_{l,m+1/2})\right)\right)\\
& + u_2|_{l,m-1/2}\left(s^{22}|_{l,m-1/2}v_2|_{l,m-1/2} + \frac{1}{2}\left(s^{12}|_{l,m}(v_1|_{l-1/2,m} + v_1|_{l+1,m})\right)\right)\\
& + u_2|_{l,m+1/2}\left(s^{22}|_{l,m+1/2}v_2|_{l,m+1/2} + \frac{1}{2}\left(s^{12}|_{l,m}(v_1|_{l-1/2,m} + v_1|_{l+1/2,m})\right)\right)\Bigg].
\end{aligned}
$$

Let now consider that $\boldsymbol{u} = \boldsymbol{v}$. We thus have

$$
\begin{aligned}
(\boldsymbol{u},\boldsymbol{u}) = \frac{1}{2}\sum_{\Omega}\Bigg[& \frac{1}{2}s^{11}|_{l-1/2,m}(u_1|_{l-1/2,m})^2 + \frac{1}{2}s^{22}|_{l,m-1/2}(u_2|_{l,m-1/2})^2 + s^{12}|_{l,m}u_1|_{l-1/2,m}u_2|_{l,m-1/2}\\
& + \frac{1}{2}s^{11}|_{l+1/2,m}(u_1|_{l+1/2,m})^2 + \frac{1}{2}s^{22}|_{l,m-1/2}(u_2|_{l,m-1/2})^2 + s^{12}|_{l,m}u_1|_{l+1/2,m}u_2|_{l,m-1/2}\\
& + \frac{1}{2}s^{11}|_{l-1/2,m}(u_1|_{l-1/2,m})^2 + \frac{1}{2}s^{22}|_{l,m+1/2}(u_2|_{l,m+1/2})^2 + s^{12}|_{l,m}u_1|_{l-1/2,m}u_2|_{l,m+1/2}\\
& + \frac{1}{2}s^{11}|_{l+1/2,m}(u_1|_{l+1/2,m})^2 + \frac{1}{2}s^{22}|_{l,m+1/2}(u_2|_{l,m+1/2})^2 + s^{12}|_{l,m}u_1|_{l+1/2,m}u_2|_{l,m+1/2}\Bigg].
\end{aligned}
$$

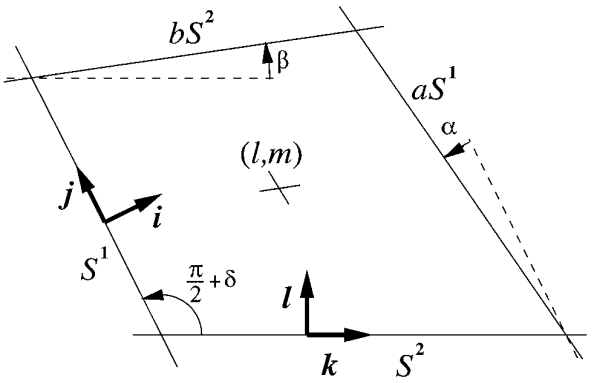

FIG. 10. Definition of the cell parameters.

It is obvious that the diagonal terms of the metric tensor s^{ii} are necessarily strictly positive. In return, the sign of both the cross terms s^{ij} $(i \neq j)$ and the products u_1u_2 are uncertain. The *positiveness* and *definiteness* is not straightforward.

In order to prove the desired result, a sufficient condition is to prove that there is some positive constant C such that

$$s^{11}(u_1)^2 + s^{22}(u_2)^2 + 2s^{12}u_1u_2 \geq C[s^{11}(u_1)^2 + s^{22}(u_2)^2] \geq 0$$

for the four terms of the sum (see Strikwerda [22, p.288]). It is equivalent to find a constant $0 \geq c \geq -1$ such that

$$cs^{11}(u_1)^2 + cs^{22}(u_2)^2 - 2s^{12}u_1u_2 \leq 0,$$

or

$$s^{11}s^{22} > (s^{12})^2.$$

We now introduce geometric conditions. A sufficient condition for the bilinear form to be definite positive is that

$$s^{11}|_{l\pm1/2,m}s^{22}|_{l,m\pm1/2} > (s^{12}|_{l,m})^2$$

is satisfied on any cell of the domain. We will only consider the condition:

$$s^{11}|_{l-1/2,m}s^{22}|_{l,m-1/2} > (s^{12}|_{l,m})^2. \tag{B.3}$$

Moreover, the variation of $\sqrt{g}$ between the adjacent cells will be neglected.

The computational cell is sketched in Fig. 10. Let us define two orthonormal basis $(\boldsymbol{i}, \boldsymbol{j})$ and $(\boldsymbol{k}, \boldsymbol{l})$ such that the vectors normal to the faces read

$$\boldsymbol{S}^1|_{l-1/2,m} = S^1\boldsymbol{i}, \quad \boldsymbol{S}^2|_{l,m-1/2} = S^2\boldsymbol{l},$$

where S^1 and S^2 are the areas of the faces.

Let δ denote the departure from orthogonality between those two faces. Then we have

$$\boldsymbol{i}\cdot\boldsymbol{k}=\boldsymbol{j}\cdot\boldsymbol{l}=\cos\delta,\quad \boldsymbol{i}\cdot\boldsymbol{l}=-\boldsymbol{j}\cdot\boldsymbol{k}=\sin\delta.$$

Let us now define the two faces $\xi^1 = l + \frac{1}{2}$ and $\xi^2 = m + \frac{1}{2}$ such that α is the angle between the face $\xi^1 = l - \frac{1}{2}$ and face $\xi^1 = l + \frac{1}{2}$, and β is the angle between the face $\xi^2 = m + \frac{1}{2}$ and face $\xi^2 = m + \frac{1}{2}$, as described in Fig. 10. Let a be the ratio of the area of two opposite faces $\xi^1 = l \pm \frac{1}{2}$ of the same cell, and let b be the ratio of the area of two opposite faces $\xi^2 = m \pm \frac{1}{2}$ for the other pair. Thus the contravariant basis vectors on these faces read

$$\boldsymbol{S}^1|_{l+1/2,m}=aS^1(\cos\alpha\boldsymbol{i}+\sin\alpha\boldsymbol{j}),\quad \boldsymbol{S}^2|_{l,m+1/2}=bS^2(\cos\beta\boldsymbol{l}+\sin\beta\boldsymbol{k}).$$

With these definitions, it is now possible to express a geometric condition for (B.3) to be satisfied. First, it is obvious that

$$s^{11}|_{l-1/2,m}s^{22}|_{l,m-1/2}=\left(\frac{S^1S^2}{\sqrt{g}}\right)^2.$$

Let us calculate the scalar $s^{12}|_{l,m}$ which is defined by

$$s^{12}|_{l,m}=\frac{1}{4g}(\boldsymbol{S}^1|_{l-1/2,m}+\boldsymbol{S}^1|_{l+1/2,m})\cdot(\boldsymbol{S}^2|_{l,m-1/2}+\boldsymbol{S}^2|_{l,m+1/2})$$

We get:

$$\begin{aligned}s^{12}|_{l,m}=\frac{S^1S^2}{4g}&((1+a\cos\alpha)(1+b\cos\beta)\sin\delta\\&+a(1+b\cos\beta)\sin\alpha\cos\delta-b(1+a\cos\alpha)\sin\beta\cos\delta\\&+ab\sin\alpha\sin\beta\sin\delta),\end{aligned}$$

or after some algebra,

$$s^{12}|_{l,m}=\frac{S^1S^2}{4g}(\sin\delta+a\sin(\delta+\alpha)+b\sin(\delta-\beta)+ab\sin(\delta+\alpha-\beta)).$$

To sum up, the geometric criterion reads

$$\sin\delta+a\sin(\delta+\alpha)+b\sin(\delta-\beta)+ab\sin(\delta+\alpha-\beta)<4.$$

Let us remark that the smaller are the three angles δ, α, and β, the better is this criterium satisfied.

ACKNOWLEDGMENTS

The authors are grateful to one of the reviewers, who pointed out the last remark of Section 3.2 and the fact that this formulation can be applied to general unstructured grids.

REFERENCES

1. Y. V. Apanovich and E. D. Lyumkis, Difference schemes for the Navier–Stokes equations on a net consisting of Dirichlet cells, *U.S.S.R. Comput. Maths. Math. Phys.* **28**(2), 57 (1988).
2. R. Aris, *Vectors, Tensors and the Basic Equations of Fluid Mechanics,* (Prentice–Hall, Englewood Cliffs, NJ, 1962).
3. R. S. Bernard and H. Kapitza, How to discretize the pressure gradient for curvilinear MAC grids, *J. Comput. Phys.* **99,** 288 (1992).
4. F. Bertagnolio and O. Daube, Velocity–vorticity formulation of the incompressible Navier–Stokes equations on nonorthogonal grids, in *Proceedings of the Third ECCOMAS Computational Fluid Dynamics Conference, Paris, France, 1996,* p. 644.
5. O. Daube, Resolution of the 2D Navier–Stokes equations in velocity–vorticity form by means of an influence matrix, *J. Comput. Phys.* **103,** 402 (1992).
6. I. Demirdzic, A. D. Gosman, R. I. Issa, and M. Peric, A calculation procedure for turbulent flow in complex geometries, *Comput. & Fluids* **15**(3), 251 (1987).
7. A. Favorskii, A. Samarskii, M. Shashkov, and V. Tishkin, Operational finite-difference schemes, *Differential Equations* **17,** 854 (1981).
8. T. B. Gatski, Review of incompressible fluid flow computations using the vorticity–velocity formulation, *Appl. Numer. Math.* **7,** 227 (1991).
9. T. B. Gatski, C. E. Grosch, and M. E. Rose, A numerical study of the two-dimensional Navier–Stokes equations in vorticity–velocity variables, *J. Comput. Phys.* **48,** 1 (1982).
10. V. Girault and P. A. Raviart, *Finite Element Methods for Navier–Stokes Equations* (Springer-Verlag, Berlin/New York, 1986).
11. R. S. Harlow and J. E. Welch, Numerical calculation of time-dependent viscous incompressible flow of fluid with free surface, *Phys. Fluids* **8,** 2182 (1965).
12. Y. Huang and U. Ghia, A multigrid method for solution of vorticity–velocity form of 3-D Navier–Stokes equations, *Commun. Appl. Numer. Methods* **8,** 707 (1992).
13. K. C. Karki, *A Calculation Procedure for Viscous Flows at all Speeds in Complex Geometries,* Ph.D. thesis, University of Minnesota, 1986.
14. G. Knorr, G. Joyce, and A. J. Marcus, *J. Comput. Phys.* **38,** 227 (1980).
15. R. A. Nicolaides, *Direct Discretisation of Planar Div-Curl Problems, ICASE Report No. 89-76,* 1989.
16. G. A. Osswald, K. N. Ghia, and U. Ghia, A direct algorithm for solution of incompressible three-dimensional unsteady Navier–Stokes equations, *AIAA Paper 87-1139,* p. 408, (1987).
17. G. Pascazio and M. Napolitano, A staggered-grid finite volume method for the vorticity–velocity equations, *Comput. & Fluids* **25**(4), (1996).
18. L. Quartapelle, *Numerical Solution of the Incompressible Navier–Stokes Equations,* (Birkhäuser, Basel, 1993). [International Series of Numerical Mathematics, Vol. 113]
19. M. Rosenfeld, D. Kwak, and M. Vinokur, A solution method for the unsteady and incompressible Navier–Stokes equations in generalized coordinate systems, *AIAA Paper 88-0718,* Reno, January 1988.

20. M. Shashkov and S. Steinberg, Support-operator finite-difference algorithms for general elliptic problems, *J. Comput. Phys.* **118,** 131 (1995).
21. W. Shyy and T. C. Vu, On the adoption of velocity variable and grid system for fluid flow computation in curvilinear coordinates, *J. Comput. Phys.* **92,** 82 (1991).
22. J. C. Strikwerda, *Finite Difference Schemes and Partial Differential Equations,* (Chapman & Hall, London/New York, 1989).
23. H. Q. Yang, S. D. Habchi, and A. J. Przekwas, General strong conservation formulation of Navier–Stokes equations in nonorthogonal curvilinear coordinates, *AIAA J.* **32**(5), 936 (1994).